Efficient Hierarchical Multiple Access for Ambient Backscatter Wireless Networks

Lanhua Li[*†], XiaoXia Huang[‡]

[*]Shenzhen Institutes of Advanced Technology, Chinese Academy of Sciences, Shenzhen, China
[†]Shenzhen College of Advanced Technology, University of Chinese Academy of Sciences, Shenzhen, China
[‡]School of Electronics and Communication Engineering, Sun Yat-Sen University, Guangzhou, China
Email: lh.li1@siat.ac.cn, huangxiaoxia@mail.sysu.edu.cn

Abstract—The ambient backscatter communication (AmBC) enables information delivery over ambient RF signals without carrier generation, and has emerged as a promising technology to build up the self-sustainable Internet-of-Things (IoT). However, when a strong ambient signal appears, multiple backscatter nodes may initiate data transmission simultaneously, causing severe contention and wasting the precious transmission opportunity. The undeterministic and sporadic nature of the ambient signal makes it a great challenge for efficient multiple access design in ambient backscatter aided wireless network (AmBWN). Moreover, the stringent energy supply and ultra low-cost design of the backscatter transmitter make most multiple access schemes no longer suitable for AmBWN. To fully share the carrier resource for backscattering, we resort to non-orthogonal multiple access (NOMA) to allow multiple devices in the same regime to transmit over the ambient signal with low latency. Moreover, we propose a hierarchical multiple access scheme which allows beamforming based spatial division multiple access among groups, and NOMA for multiple users access within a group. The evaluation result shows that latency and SINR can be significantly improved with minimal overhead at the transmitter.

I. INTRODUCTION

The Internet-of-Things (IoT) has been widely deployed in various applications, such as logistics, industrial, healthcare, smart homes or cities, and environment monitoring. Most wireless IoT devices are powered by recharging or battery replacement which costs tremendous labor or expenditure. So the energy supply and sustainability have long been deemed as the most important problems for further applications of IoT. Recently, the low-power and low-cost ambient backscatter communication (AmBC), which allows the node to deliver information by reflecting and modulating incident RF signal, has been introduced as a promising technology for power constrained wireless networks. The ambient backscatter node typically consumes power orders of magnitude less than the conventional radio.

However, every coin has its two sides. Without a persistent and stable carrier, the availability of the transmission opportunity for the AmBC node is highly volatile and dependent on the strength of the environmental signal. Once a strong environmental signal appears, many backscatter nodes may initiate the data transmission immediately to grasp the precious transmission opportunity, causing heavy collisions and wasting communication resources. The frequent collision results in unpredictable latency, and poor energy efficiency and throughput performance. Traditional multiple access schemes, such as FDMA, CDMA and TDMA, introduce high power consumption or high protocol complexity, or require strict synchronization among nodes. Therefore, those schemes are not suitable for low-cost ambient backscatter nodes (BNs), and even adversely increase the power consumption without performance guarantee.

Therefore, the undeterministic and sporadic nature of the ambient signal and the low cost demand on the backscatter transmitter are two main challenges for efficient multiple access scheme design in ambient backscatter aided wireless network (AmBWN). To tackle these challenges, we propose a hierarchical multiple access scheme to reduce latency and improve throughput in AmBWN. The hierarchical multiple access scheme consists of the power-domain non-orthogonal multiple access (NOMA) for multiple users access within a group, i.e. the intra-group NOMA, and beamforming based spatial division multiple access among groups, i.e. the inter-group beamforming. By exploiting the difference of signal strength in the power domain, NOMA can simultaneously serve multiple users and improve spectrum efficiency and latency. To ensure the effectiveness of NOMA, we could proactively control the reflection coefficient at each BN to optimize the received signal strength at access point (AP) from a group of BNs. Moreover, with a beamforming scheme, the multi-antenna AP can support simultaneous access of multiple groups by sharing the ambient signal in the space domain. Considering the inter-group interference, we further investigate the optimal grouping strategy to mitigate the interference and improve the aggregate capacity of all users. In particular, we formulate a max-min group throughput optimization problem which realizes the tradeoff between total throughput and fairness. Meanwhile, a hierarchical scheduling algorithm is presented to solve the complex optimization problem. Shifting the computation complexity of the beamforming and interference cancellation in NOMA to the AP, the proposed multiple access scheme is affordable for AmBWN without increasing the overhead of the backscatter transmitters.

The rest of this paper is organized as follows. We briefly review the related works in Section II. After that, we introduce the hierarchical multiple access control model in

Section III, and then presents the design details of the joint NOMA and beamforming multiple access scheme in Section IV. Simulation results and conclusions are summarized in Section V and VI, respectively.

II. RELATED WORK

By leveraging the RF signal resources in the environment, it is promising to realize the sustainable IoT networks through the ultra-low power AmBC combined with RF based energy harvesting technology. In [1], the tag-to-tag AmBC system is first introduced to enable two batteryless devices to communicate using ambient TV signals, consuming only 0.25μW at the transmitter and 0.54μW at the receiver. But the transmission range is limited to two feet with the data rate no greater than 10kbps. To overcome this limitation, a number of backscattering schemes are proposed to improve the transmission range and data rate, such as the turbocharging backscatter [2], the passive Wi-Fi [3], the FM backscatter [4] and the LoRa backscatter [5].

Dealing with the undedicated ambient RF signal, some works focus on the modulation and detection design to reduce the bit error rate (BER) at the backscatter receiver. In [6] and [7], the maximum likelihood based noncoherent detection is adopted to support the ASK and FSK modulation in the AmBC system. The coherent detection has been further studied in [8] and [9] for the PSK modulation. To avoid sending pilot symbols for channel estimation, Ma et al. [10] propose a blind channel estimator based on the expectation maximization estimation algorithm to obtain the channel parameters. In [11], Yang et al. recover information from both ambient backscatter signal and the RF source by utilizing the maximum-likelihood detector as well as the successive interference-cancellation based detector. Moreover, detection performance can be enhanced using multiple receiver antennas [2, 12, 13].

There are a few works investigating the multiple access problem in backscatter communication networks. In [14], Bletsas et al. jointly adopt directional beamforming at the reader and frequency shift keying modulation at the tags to mitigate the collision. In [15], Wang et al. propose an interesting compressive sensing algorithm for collision avoidance by treating bursty backscatter transmissions as a sparse code. Moreover, the power sparsity of AmBC is utilized in [16] to support NOMA as well as M-ary modulation for concurrent backscatter transmissions. To support multiple access in full-duplex backscatter communication networks, a time-hopping spread spectrum based multiple access scheme performs sequence-switch modulation at each reader and enables the non-coherent detection at the tags [17]. In addition, Guo et al. propose the multiplexing scheme in different regions or with different backscattered power levels to achieve NOMA in the backscatter communication system [18].

III. HIERARCHICAL MULTIPLE ACCESS MODEL FOR AmBWN

In this section, we introduce a hierarchical multiple access control model for AmBWN, as shown in Fig. 1. At the high layer, beamforming is performed upon receiving signals from all groups perspective. At the low layer, we apply the NOMA with Successive Interference Cancellation (SIC) to decode the received backscattering signal in each group separately.
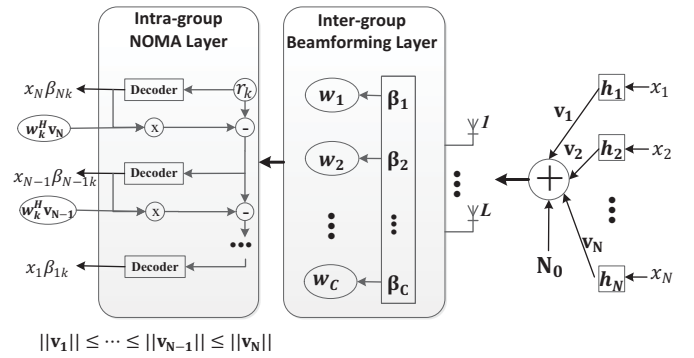

Fig. 1. The system model for AmBWN with N BNs and an AP. Each BN is equipped with a single transmitting antenna and the AP has L receiving antennas.

A. System Model

We consider the uplink transmission from the BN to AP. The set of BNs is denoted by $\mathcal{N} = \{1, 2, \ldots, N\}$, which is arbitrarily deployed and tuned to the same frequency band. The AP is equipped with L antennas and performs beamforming and SIC to support multiple concurrent transmissions over the same frequency. Since the strength and data rate of the ambient RF source is much higher compared to the backscattering signals, the AP is able to filter out the ambient RF signal [1, 19].

The BN contains an antenna which is shared by a RF energy harvester, a backscatter transmitter and a signal processor. The RF energy harvester converts RF signals to DC current, which can be stored in a rechargeable battery. The backscatter transmitter changes the impedance according to the information bit, realizing on-off keying modulation or other advanced modulation schemes. Let α_i, s_i, and b_i denote the reflection coefficient of the i-th BN, the perceived ambient RF signal at BN_i, and the information bit of BN_i, respectively. The refection coefficient specifies the portion of the power of an incident signal reflected by a BN for backscatter transmission. A reflection coefficient of 0 indicates that an incident signal is completely absorbed for reception or energy harvesting. Whereas, a reflection coefficient of 1 means that the antenna completely reflects the incident signal for backscatter transmission. The transmission vector of BNs is denoted by $\mathbf{X} \triangleq [x_1, x_2, \ldots, x_N]^T \in \mathbb{C}^{N \times 1}$ with $x_i = \sqrt{\alpha_i} s_i b_i$. We define the channel matrix as $\mathbf{H} \triangleq [\mathbf{h_1}, \mathbf{h_2}, \ldots, \mathbf{h_N}] \in \mathbb{C}^{L \times N}$, where $\mathbf{h_i}$ denotes the channel response from BN_i to the AP. We assume that $\mathbf{H}$ are fixed during each transmission block

and change independently from one block to another. Note that the backscatter channel can be estimated with a preamble [20].

B. Inter-Group Beamforming

At the inter-group beamforming layer, the AP divides the received signals into C (C≤ L) groups, then performs beamforming to the grouped signals. We sort the BNs with the received backscattering signal, $\mathbf{v_i} = \mathbf{h_i} s_i$, which accounts for the impact of BN's channel gain as well as the strength of the ambient signal. The BNs are sorted in the ascending order of their received backscattering signals as $||\mathbf{v_1}|| \leqslant ||\mathbf{v_2}|| \leqslant \ldots \leqslant ||\mathbf{v_N}||$. Let us define a variable β_{ij} which indicates whether BN$_i$ belongs to the j-th group or not. When β_{ij} equals 1, BN$_i$ is selected by the j-th group. The j-th group vector is denoted by $\boldsymbol{\beta_j} \triangleq [\beta_{1j}, \beta_{2j}, \ldots, \beta_{Nj}]^T \in \mathbb{C}^{N \times 1}$. Then the grouping matrix is given by $\boldsymbol{\beta} \triangleq [\boldsymbol{\beta_1}, \boldsymbol{\beta_2}, \ldots, \boldsymbol{\beta_C}] \in \mathbb{C}^{N \times C}$. The beamforming matrix is defined as $\mathbf{W} \triangleq [\mathbf{w_1}, \mathbf{w_2}, \ldots, \mathbf{w_C}] \in \mathbb{C}^{L \times C}$, where $\mathbf{w_i}$ denotes the beamforming vector for i-th group with $||\mathbf{w_i}|| = 1$. After applying beamforming to the received signals, the output signal vector of groups, $\mathbf{r} = [r_1, r_2, \ldots, r_C]^T$, is

$$\mathbf{r} = \mathbf{W^H H} D(\mathbf{X}) \boldsymbol{\beta} \mathbf{1}_C + \mathbf{W^H N_0}, \tag{1}$$

where $\mathbf{N_0}$ is the received noise vector at the AP. We define $D(\cdot)$ to construct a diagonal matrix with the given vector, and let $\mathbf{1}_M$ denotes a $M \times 1$ vector with all elements being one. From (1), the signal of the k-th group is

$$r_k = \sum_{j=1}^{C} \sum_{i=1}^{N} \mathbf{w_k^H h_i} \sqrt{\alpha_i} s_i b_i \beta_{ij} + n_0, \tag{2}$$

and n_0 is the additive Gaussian noise which is assumed to be independent Gaussian random variable with zero mean and variance σ^2.

C. Intra-Group NOMA

Intra-group NOMA with SIC receiver at AP processes the received signals in the same group by a descending order from the strongest signal to the weakest signal. First, it decodes the strongest signal and treats the signal from all other BNs in the same group as interference. Once the strongest signal is successfully decoded, it is extracted from the received signal of the group. As such, the SIC receiver then decodes the second strongest signal and so on. After applying SIC to the k-th group of signals and retrieving signals stronger than the m-th strongest signal, the residual signal in the k-th group is

$$r_{mk} = \mathbf{w_k^H v_m} \sqrt{\alpha_m} b_m \beta_{mk} + \sum_{i=1}^{m-1} \mathbf{w_k^H v_i} \sqrt{\alpha_i} b_i \beta_{ik}$$
$$+ \sum_{j \in \mathcal{C} \setminus k} \sum_{i=1}^{N} \mathbf{w_k^H v_i} \sqrt{\alpha_i} b_i \beta_{ij} + n_0. \tag{3}$$

On the right side of (3), the first term is the desired signal from BN$_m$. The second term is the intra-group interference

from the BNs in the same group k, and the third term is the inter-group interference from all the BNs in the other group.

Given $\mathbb{E}[|s_m|^2] = P_m$ and $\mathbb{E}[|b_m|^2] = 1$, respectively. $\mathbb{E}[\cdot]$ stands for the expectation operation. Then according to (3), the power of BN$_m$ in k-th group is

$$\phi_{mk} = |\mathbf{w_k^H h_m}|^2 \alpha_m P_m \beta_{mk}, \tag{4}$$

and BN$_m$'s intra-group interference power is

$$N_{mk}^{intra} = \sum_{i=1}^{m-1} \phi_{ik} = \sum_{i=1}^{m-1} |\mathbf{w_k^H h_i}|^2 \alpha_i P_i \beta_{ik}. \tag{5}$$

Moreover, each BN in the same group experiences the same interference from all other groups at the AP. The inter-group interference power of k-th group is expressed as follows

$$N_k^{inter} = \sum_{j \in \mathcal{C} \setminus k} \sum_{i=1}^{N} |\mathbf{w_k^H h_i}|^2 \alpha_i P_i \beta_{ij}. \tag{6}$$

IV. JOINT NOMA AND BEAMFORMING BASED MULTIPLE ACCESS SCHEME

The power-domain NOMA achieves low latency and high capacity via simultaneously serving multiple users with minimal interference. According to the SIC mechanism, a large disparity in signal strength can efficiently suppress the interference among BNs. The acquisition of different perceived power within a group lies in the proper grouping and the reflection coefficient control related to the transmission power of a BN. Beamforming is capable of sharing the resource among groups in the spatial domain to improve the total capacity. But space sharing will inevitably introduce the inter-group interference. Hence, the beamforming and grouping are jointly taken into consideration to decrease the inter-group interference.

Motivated by these considerations, we first formulate the max-min group throughput optimization problem to obtain a tradeoff between sum-throughput and fairness via seeking the optimal grouping, beamforming matrix and reflection coefficient. Further, to solve the complex optimization problem, a new hierarchical scheduling algorithm is presented by developing a less complex grouping and forming the corresponding beamforming matrix, and then optimizing the reflection coefficient of each BN.

A. Max-Min Group Throughput Optimization Problem

The received SINR of BN$_m$ in k-th group is given by

$$\begin{aligned} \text{SINR}_{mk} &= \frac{\phi_{mk}}{N_{mk}^{intra} + N_k^{inter} + \sigma^2} \\ &= \frac{|\mathbf{w_k^H h_m}|^2 \alpha_m P_m \beta_{mk}}{\sum_{i=1}^{m-1} \phi_{ik} + \sum_{j \in \mathcal{C} \setminus k} \sum_{i=1}^{N} |\mathbf{w_k^H h_i}|^2 \alpha_i P_i \beta_{ij} + \sigma^2}, \end{aligned} \tag{7}$$

Then the total throughput of k-th group is

$$
\begin{aligned}
R_k &= \sum_{i=1}^{N} B \log_2(1 + \text{SINR}_{ik}) \\
&= B \log_2[(1 + \frac{\phi_{1k}}{N_k^{inter} + \sigma^2})(1 + \frac{\phi_{2k}}{\phi_{1k} + N_k^{inter} + \sigma^2}) \\
&\quad \dots (1 + \frac{\phi_{Nk}}{\sum_{i=1}^{N-1} \phi_{ik} + N_k^{inter} + \sigma^2})] \\
&= B \log_2(1 + \frac{\sum_{i=1}^{N} \phi_{ik}}{N_k^{inter} + \sigma^2}),
\end{aligned}
\tag{8}
$$

where B is the bandwidth.

We formulate the max-min group throughput optimization problem by jointly considering the grouping $\boldsymbol{\beta}$, beamforming matrix $\mathbf{W}$, and reflection coefficient $\boldsymbol{\alpha} \triangleq [\alpha_1, \alpha_2, \dots, \alpha_N]$ as follows

$$
\max_{\boldsymbol{\alpha}, \boldsymbol{\beta}, \mathbf{W}} \quad \min_{1 \leqslant k \leqslant C} R_k \tag{9a}
$$

$$
s.t. \quad E_i - P_i^c \geqslant 0, \ \forall i \in \mathcal{N}, \tag{9b}
$$

$$
\sum_{j=1}^{C} \beta_{ij} = 1, \ \forall i \in \mathcal{N}, \tag{9c}
$$

$$
\beta_{ik} \in \{0, 1\}, \alpha_i \in [0, 1], ||\mathbf{w_k}|| = 1, \forall k \in \mathcal{C}, \forall i \in \mathcal{N}, \tag{9d}
$$

where (9a) defines the minimum group throughput. The energy consumption of BN_i is limited by the energy storage E_i in (9b) with the power consumption given in (10). Constraint (9c) ensures that each BN can only be assigned to one of the groups.

Besides, since a BN can perform backscattering and energy harvesting simultaneously by controlling the reflection coefficient, we consider the net power consumption with the harvested energy. The power consumption of BN_i is given by

$$
P_i^c = P_c - \eta_0 (1 - \alpha_i) P_i, \tag{10}
$$

where P_c denotes the total power consumption of encoding, modulation and other operations during the data transmission, and η_0 is the power conversion efficiency.

B. Hierarchical Scheduling Algorithm

Given the problem formulation in (9a)-(9d), the optimal grouping problem is a 0-1 mixed integer non-linear programming (MINLP), which is NP-hard in general. The problem becomes computationally unaffordable for the densely deployed AmBWN. Therefore, we propose a efficient hierarchical scheduling algorithm to solve the problem in three stages. In the first stage, we derive a less complex grouping strategy by exploiting the disparity of backscattering signal gains among BNs and the orthogonality among BNs' channels. In the second stage, the grouping is fixed, and the corresponding beamforming matrix is identified. Finally, we fix the grouping and beamforming matrix, and find the optimal reflection coefficient of all nodes.

1) Grouping Strategy. According to the group throughput defined in (8), the perceived power from the group members and the inter-group interference are the two factors determining the group throughput.

The perceived power of each BN depends on its received backscattering signal and reflection coefficient. In a group, the BN with the highest backscattering signal does not interfere with BNs with weaker backscattering signal by employing perfect SIC. Therefore, this BNs can transmit with its energy-affordable maximum reflection coefficient to achieve high throughput. Thus, it is beneficial to distribute the BNs with high backscattering signal into different groups, as they can significantly contribute to the throughput of a group.

The inter-group interference determined by the orthogonality among the BNs' channels in different groups. If the BNs' channels in a group are nearly orthogonal to the channels of the BNs in other groups, the inter-group interference $\sum_{j \in \mathcal{C} \backslash k} \sum_{i=1}^{N} |\mathbf{w_k^H h_i}|^2 \beta_{ij}$ decreases. Hence, those BNs nearly orthogonal to each other should be selected to different groups to migrate the inter-group interference.

Based on this criterion, we propose the following grouping strategy. First, the BNs are sorted in the ascending order of received backscattering signals $\mathbf{V}$. The number of groups is predefined as K. Then, if the number of BNs N is divisible with K, the sorted BNs are uniformly divided into $\delta = \lfloor N/K \rfloor$ number of sets $\mathbf{S} \triangleq [S_1, S_2, \dots, S_\delta]$ with $S_i = \{\text{BN}_{N-(i-1)K}, \text{BN}_{N-(i-1)K-1}, \dots, \text{BN}_{N-iK+1}\}$, where $\lfloor \cdot \rfloor$ denotes the floor function. Otherwise, the set size δ is equal to $\lfloor N/K \rfloor + 1$ with the remaining BNs assigned to the last set S_δ. Finally, the BNs are selected into groups based on their backscattering signal and channels' orthogonality. The BNs in the first set S_1 are uniformly distributed to K groups. Then, we select the BNs from other sets which are least orthogonal to current BN into the same group. For example, if BN_q in set S_i is assigned to the q-th group, BN_{p_j} in set S_j will be selected to the q-th group if it satisfies,

$$
p_j^* = \min \frac{|\mathbf{h_q} \cdot \mathbf{h_{p_j}}|}{|\mathbf{h_q}||\mathbf{h_{p_j}}|}, \forall p_j \in S_j, \text{ where } j \neq i. \tag{11}
$$

Then, $\text{BN}_{p_i^*}$ will be chosen by the q-th group and the grouping variable $\beta_{p_i^* q}$ will be set to 1.

2) Beamforming. Next we consider the beamforming among groups. Let $\mathbf{H_c} = \mathbf{H}\boldsymbol{\beta}$ denote the grouping channel matrix. Since the grouping matrix $\boldsymbol{\beta}$ has been determined in the first stage, the beamforming matrix can be updated according to zero-forcing (ZF) criterion as follows

$$
\mathbf{W} = (\mathbf{H_c^H H_c})^{-1} \mathbf{H_c^H}. \tag{12}
$$

3) Optimal Reflection Coefficient. Given the grouping and beamforming matrix, we derive the optimal reflection coefficient for the AmBWN. Denote G as the minimum group throughput. The problem in (9) can be expanded and rewritten as

$$
\max_{\boldsymbol{\alpha}} \quad G \tag{13a}
$$

$$s.t. \quad B\log_2\left(1 + \frac{\sum_{i=1}^{N} \zeta_{ik}\beta_{ik}\alpha_i}{\sum_{j\in\mathcal{C}\backslash k}\sum_{n=1}^{N}\zeta_{nk}\beta_{nj}\alpha_n + \sigma^2}\right) \geq G, \forall k \in \mathcal{C}, \tag{13b}$$

$$E_i - (P_c - \eta_0 P_i + \alpha_i \eta_0 P_i) \geq 0, \ \forall i \in \mathcal{N}, \tag{13c}$$

$$\alpha_i \in [0,1], \ \forall i \in \mathcal{N}, \tag{13d}$$

where $\zeta_{ik} = |\mathbf{w_k^H h_i}|^2 P_i$. The above problem is convex, which can be solved efficiently.

V. NUMERICAL RESULTS

We evaluate the performance of the proposed joint beamforming and NOMA (B-NOMA) multiple access scheme for AmBWN. The BNs are uniformly deployed in $100 \times 100m^2$ area and operating in the 2.4GHz band. The bandwidth of each signal is 10MHz. The ambient signals appear over non-overlapping frequencies. The channel power gain is modeled as $\mathbf{h_i} = \mathbf{g_i}d_i^{-\alpha_h}$, where $\mathbf{g_i}$ is Rayleigh fading which follows a complex Gaussian distribution with zero mean and -45dBm variance. Let d_i denote the distance between the BN_i and the AP, and the path loss exponent α_h is 4. The power of the ambient signal follows Gaussian process with mean μ_p in the range of [-30dBm, 0dBm], which is randomly selected for each simulation. The variance of the ambient signal σ_p is -45dBm. The simulation parameters are summarized in Table I.

TABLE I
SIMULATION PARAMETERS

Parameters	Value
Number of BNs	[20, 40, 60, 80, 100]
Number of ambient signals	[1, 2, 4]
Receiver noise density	-174dBm/Hz
Power consumption for backscatter transmission (P_c)	0.25μW [2]
Power conversion efficiency (η_0)	0.7 [21]

1) Comparison of Two Schemes. We compare the performance of the proposed B-NOMA with the dynamic user clustering for uplink NOMA (labeled as D-NOMA) [22] in terms of BN's average signal-to-interference-plus-noise ratio (SINR) and average delay. In D-NOMA, the grouping strategy is based on the distinctness of the channel gain. Meanwhile, D-NOMA assumes that each group operates over a channel orthogonal to other channels. This implies that inter-group interference can be neglected in D-NOMA. We compare the performance of the two schemes with respect to different number of BNs, in presence of 1, 2 and 4 ambient signals over different frequencies.

Fig. 2 shows the average SINR when the number of BNs varies from 20 to 100. B-NOMA improves the average SINR by 2.67 times, 3.34 times and 3.45 times compared to D-NOMA with respect to 1, 2 and 4 ambient signals. In B-NOMA, the hierarchical multiple access jointly takes the advantages of beamforming and grouping in the space domain, which can efficient suppress the interference among BNs, and thus achieves significantly improved SINR. As the number of BNs increases, the interference becomes significant and can no longer be avoided by beamforming, leading to reduced SINR.
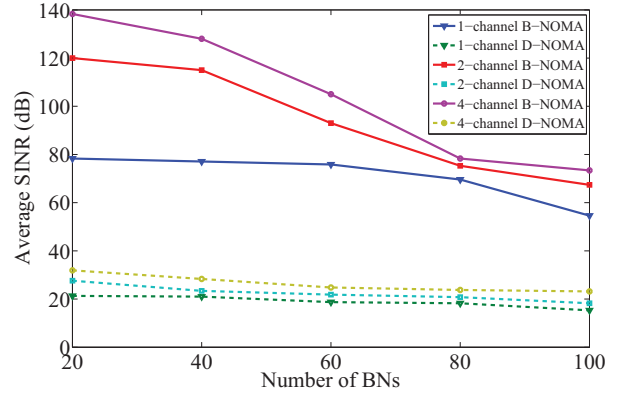

Fig. 2. Average SINR vs. number of BNs.

The average delay with respect to the number of BNs is shown in Fig. 3. It is observed that B-NOMA achieves much lower average delay than D-NOMA. Given 1, 2 and 4 ambient signals, B-NOMA can decrease the average delay by 83.3%, 92.6% and 92.1% compared to D-NOMA when the number of BNs reaches 100. This stems from the fact that B-NOMA ensures fairness via the scheduling algorithm, which can effectively reduce the delay of BNs with weak channel gains and then decrease the average delay. Besides, when the number of ambient signals increases, the delay of B-NOMA grows more slowly than that of D-NOMA. This is because more ambient signals over different frequencies offers more carriers for backscattering. So the contention becomes moderate, inhibiting the overall growth of delay.
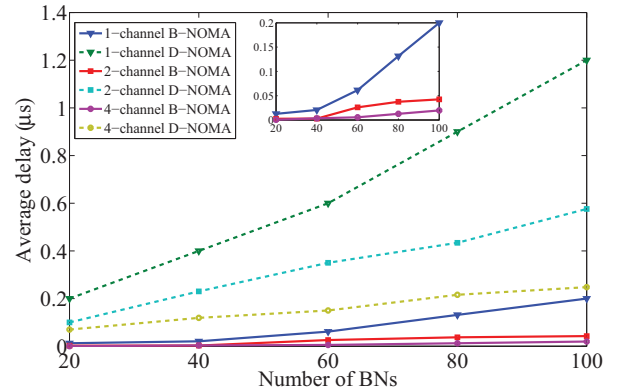

Fig. 3. Average delay vs. number of BNs.

2) Impact of ambient signal power. Fig. 4 shows the sum-throughput when the average power of the ambient signal μ_p increases from -30dBm to 0dBm given different group sizes. When μ_p increases, the sum throughput first grows and then becomes relatively stable at about 14.2Mbps, 17.1Mbps, 12.2Mbps, and 11.4Mbps with respect to 3-user, 6-user, 9-user and 12-user groupings. As the ambient signal power further increases, the interference among BNs suppresses the growth in throughput. It is also observed that the 6-user B-NOMA achieves the highest sum throughput, whereas the

12-user B-NOMA attains the worst throughput. This implies that the total throughput can be improved by appropriately determining the number of users within a group, but the throughput of B-NOMA deteriorates if the group size increases beyond a certain threshold and results in the increased intra-group interference.
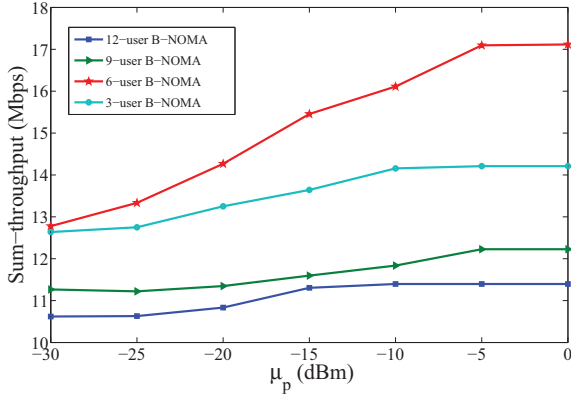

Fig. 4. Sum throughput vs. average of ambient signal power.

VI. CONCLUSIONS

In this paper, we propose an efficient hierarchical multiple access scheme, i.e. B-NOMA, which supports power-domain NOMA within a group and beamforming based spatial division multiple access among groups in AmBWN. B-NOMA supports multiple concurrent transmissions over the ambient RF signal and effectively combats against the randomness and intermittence of the ambient signal which is precious carrier for backscattering. As the computation complicated beamforming and SIC receiving are performed at the AP, B-NOMA fits the low-power and low-cost ambient backscatter nodes well. In particular, the proposed B-NOMA takes the fairness into consideration via the max-min group throughput optimization, which is solved by a hierarchical scheduling algorithm. Compared with D-NOMA, B-NOMA can achieve significantly decreased latency and impressive SINR performance.

REFERENCES

[1] V. Liu, A. Parks, V. Talla, S. Gollakota, D. Wetherall, and J. R. Smith, "Ambient backscatter: wireless communication out of thin air," in *proc. ACM SIGCOMM*, vol. 43, no. 4, Hong Kong, China, Aug. 2013, pp. 39–50.

[2] A. N. Parks, A. Liu, S. Gollakota, and J. R. Smith, "Turbocharging ambient backscatter communication," in *proc. ACM SIGCOMM*, vol. 44, no. 4, Chicago, Illinois, USA, Aug. 2014, pp. 619–630.

[3] B. Kellogg, V. Talla, S. Gollakota, and J. R. Smith, "Passive Wi-Fi: Bringing low power to Wi-Fi transmissions," in *proc. USENIX NSDI*, Santa Clara, CA, Jul. 2016, pp. 151–164.

[4] A. Wang, V. Iyer, V. Talla, J. R. Smith, and S. Gollakota, "FM backscatter: Enabling connected cities and smart fabrics." in *proc. USENIX NSDI*, Boston, MA, USA, Jul. 2017, pp. 243–258.

[5] V. Talla, M. Hessar, B. Kellogg, A. Najafi, J. R. Smith, and S. Gollakota, "LoRa backscatter: Enabling the vision of ubiquitous connectivity," *ACM Interact. Mob. Wearable Ubiquitous Technol. (IMWUT)*, vol. 1, no. 3, pp. 105:1–105:24, 2017.

[6] G. Wang, F. Gao, Z. Dou, and C. Tellambura, "Uplink detection and BER analysis for ambient backscatter communication systems," in *proc. IEEE GLOBECOM*, San Diego, CA, USA, Dec. 2015, pp. 1–6.

[7] J. Qian, F. Gao, G. Wang, S. Jin, and H. B. Zhu, "Noncoherent detections for ambient backscatter system," *IEEE Trans. Wireless Commun.*, vol. 16, no. 3, pp. 1412–1422, 2017.

[8] N. Fasarakis-Hilliard, P. N. Alevizos, and A. Bletsas, "Coherent detection and channel coding for bistatic scatter radio sensor networking," *IEEE Trans. Commun.*, vol. 63, no. 5, pp. 1798–1810, 2015.

[9] J. Qian, F. Gao, G. Wang, S. Jin, and H. Zhu, "Semi-coherent detection and performance analysis for ambient backscatter system," *IEEE Trans. Commun.*, vol. 65, no. 12, pp. 5266–5279, 2017.

[10] S. Ma, G. Wang, R. Fan, and C. Tellambura, "Blind channel estimation for ambient backscatter communication systems," *IEEE Commun. Lett.*, vol. 22, no. 6, pp. 1296–1299, 2018.

[11] G. Yang, Q. Zhang, and Y.-C. Liang, "Cooperative ambient backscatter communications for green internet-of-things," *IEEE Internet of Things Journal*, vol. 5, no. 2, pp. 1116–1130, 2018.

[12] Z. Mat, T. Zeng, G. Wang, and F. Gao, "Signal detection for ambient backscatter system with multiple receiving antennas," in *proc. IEEE CWIT*, St. John's, NL, Canada, Jul. 2015, pp. 50–53.

[13] G. Yang and Y.-C. Liang, "Backscatter communications over ambient OFDM signals: Transceiver design and performance analysis," in *proc. IEEE GLOBECOM*, Washington, DC, USA, Dec. 2016, pp. 1–6.

[14] A. Bletsas, S. Siachalou, and J. N. Sahalos, "Anti-collision backscatter sensor networks," *IEEE Trans. Wireless Commun.*, vol. 8, no. 10, pp. 5018–5029, 2009.

[15] J. Wang, H. Hassanieh, D. Katabi, and P. Indyk, "Efficient and reliable low-power backscatter networks," in *proc. ACM SIGCOMM*, Helsinki, Finland, Aug. 2012, pp. 61–72.

[16] T. Kim and D. Kim, "Novel sparse-coded ambient backscatter communication for massive iot connectivity. arxiv 2018," *arXiv preprint arXiv:1806.02975*.

[17] W. Liu, K. Huang, X. Zhou, and S. Durrani, "Full-duplex backscatter interference networks based on time-hopping spread spectrum," *IEEE Trans. Wireless Commun.*, vol. 16, no. 7, pp. 4361–4377, 2017.

[18] J. Guo, X. Zhou, S. Durrani, and H. Yanikomeroglu, "Design of non-orthogonal multiple access enhanced backscatter communication," *IEEE Trans. Wireless Commun.*, vol. 17, no. 10, pp. 6837–6852, 2018.

[19] B. Kellogg, A. Parks, S. Gollakota, J. R. Smith, and D. Wetherall, "Wi-Fi backscatter: Internet connectivity for RF-powered devices," in *proc. ACM SIGCOMM*, Chicago, Illinois, USA, Aug. 2014, pp. 17–22.

[20] D. Bharadia, K. R. Joshi, M. Kotaru, and S. Katti, "BackFi: High throughput WiFi backscatter," in *proc. ACM SIGCOMM*, London, United Kingdom, Aug. 2015, pp. 283–296.

[21] J.-Y. Park, S.-M. Han *et al.*, "A rectenna design with harmonic-rejecting circular-sector antenna," *IEEE Antennas and Wireless Propagation Letters*, vol. 3, pp. 52–54, 2004.

[22] M. S. Ali, H. Tabassum, and E. Hossain, "Dynamic user clustering and power allocation for uplink and downlink non-orthogonal multiple access (noma) systems," *IEEE Access*, vol. 4, pp. 6325–6343, 2016.